Light-Emitting Organic Materials with Variable Charge Injection and Transport Properties

Andrew C.-A. Chen, Jason U. Wallace, Simon K.-H. Wei, Lichang Zeng, and Shaw H. Chen*

Department of Chemical Engineering and Laboratory for Laser Energetics, 240 East River Road, University of Rochester, Rochester, New York 14623-1212

Thomas N. Blanton

Research and Development Laboratories B82, Eastman Kodak Company, Rochester, New York 14650-2106

Received August 30, 2005. Revised Manuscript Received November 4, 2005

Novel light-emitting organic materials comprising conjugated oligomers chemically attached via a flexible spacer to an electron- or hole-conducting core were designed for tunable charge injection and transport properties. Representative glassy-isotropic and glassy-liquid-crystalline (i.e., noncrystalline solid) materials were synthesized and characterized; they were found to exhibit a glass transition temperature and a clearing point close to 140 and 250 °C, respectively; an orientational order parameter of 0.75; a photoluminescence quantum yield up to 51%; and HOMO and LUMO energy levels intermediate between those of blue-emitting oligofluorenes and the ITO and Mg/Ag electrodes commonly used in organic light-emitting diodes, OLEDs. This class of materials will help to balance charge injection and transport and to spread out the charge recombination zone, thereby significantly improving the device efficiency and lifetime of unpolarized and polarized OLEDs.

I. Introduction

Since the discovery of efficient electroluminescence at a relatively low voltage using organic materials, including low-molar-mass fluorescent dyes[1] and π-conjugated polymers,[2] intensive efforts have been devoted to improving the efficiency and lifetime of organic light-emitting diodes (OLEDs). Whereas low-molar-mass materials can be deposited as thin films by sublimation, conjugated polymers can be readily processed into large-area thin films by spin-coating from dilute solutions. In principle, electrons and holes are injected from the cathode and anode, respectively, for the formation of excitons in the emissive layer where radiative decay takes place. To achieve a high quantum yield with a long device lifetime, it is crucial that charge injection and transport be balanced and that the recombination zone be spread out in space. Four strategies have been reported in the literature: (i) using a low-work-function metal as the cathode, such as Ca or Ba capped with Al or Ag;[3−6] (ii) adding an injection, a buffer, and/or a charge-transport layer;[7−20] (iii) physically blending an emissive material with a charge-transporting material;[21−36] and (iv) chemically

* To whom correspondence should be addressed. E-mail: shch@lle.rochester.edu.

(1) Tang, C. W.; VanSlyke, S. A. *Appl. Phys. Lett.* **1987**, *51*, 913.
(2) Burroughes, J. H.; Bradley, D. D. C.; Brown, A. R.; Marks, R. N.; Mackay, K.; Friend, R. H.; Burns, P. L.; Holmes, A. B. *Nature* **1990**, *347*, 539.
(3) Gustafsson, G.; Cao, Y.; Treacy, G. M.; Klavetter, F.; Colaneri, N.; Heeger, A. J. *Nature* **1992**, *357*, 477.
(4) Cao, Y.; Yu, G.; Parker, I. D.; Heeger, A. J. *J. Appl. Phys.* **2000**, *88*, 3618.
(5) Ego, C.; Grimsdale, A. C.; Uckert, F.; Yu, G.; Srdanov, G.; Müllen, K. *Adv. Mater.* **2002**, *14*, 809.
(6) Martens, H. C. F.; Huiberts, J. N.; Blom, P. W. M. *Appl. Phys. Lett.* **2000**, *77*, 1852.
(7) Adachi, C.; Tokito, S.; Tsutsui, T.; Saito, S. *Jpn. J. Appl. Phys.* **1988**, *27*, L269.
(8) Adachi, C.; Tsutsui, T.; Saito, S. *Appl. Phys. Lett.* **1989**, *55*, 1489.
(9) Brown, A. R.; Bradley, D. D. C.; Burroughes, J. H.; Friend, R. H.; Greenham, N. C.; Burn, P. L.; Holmes, A. B.; Kraft, A. *Appl. Phys. Lett.* **1992**, *61*, 2793.
(10) Yang, Y.; Pei, Q. *J. Appl. Phys.* **1995**, *77*, 4807.
(11) Strukelj, M.; Miller, T. M.; Papadimitrakopoulos, F.; Son, S. *J. Am. Chem. Soc.* **1995**, *117*, 11976.
(12) Buchwald, E.; Meier, M.; Karg, S.; Poesch, P.; Schmidt, H. W.; Strohriegel, P.; Riess, W.; Schwoerer, M. *Adv. Mater.* **1995**, *7*, 839.
(13) Fukuda, T.; Kanbara, T.; Yamamoto, T.; Ishikawa, K.; Takezoe, H.; Fukuda, A. *Appl. Phys. Lett.* **1996**, *68*, 2346.
(14) Kim, Y.; Bae, K. H.; Jeong, Y. Y.; Choi, D. K.; Ha, C. S. *Chem. Mater.* **2004**, *16*, 5051.
(15) Liew, Y.-F.; Zhu, F.; Chua, S.-J.; Tang, J.-X. *Appl. Phys. Lett.* **2004**, *85*, 4511.
(16) Liao, C.-H.; Lee, M.-T.; Tsai, C.-H.; Chen, C. H. *Appl. Phys. Lett.* **2005**, *86*, 203507.
(17) Yi, Y.; Kang, S. J.; Cho, K.; Koo, J. M.; Han, K.; Park, K.; Noh, M.; Whang, C. N.; Jeong, K. *Appl. Phys. Lett.* **2005**, *86*, 213502.
(18) Choi, H. W.; Kim, S. Y.; Kim, W.-K.; Lee, J.-L. *Appl. Phys. Lett.* **2005**, *87*, 082102.
(19) Kim, S. Y.; Baik, J. M.; Yu, H. K.; Kim, K. Y.; Tak, Y.-H.; Lee, J.-L. *Appl. Phys. Lett.* **2005**, *87*, 072105.
(20) Hong, I.-H.; Lee, M.-W.; Koo, Y.-M.; Jeong, H.; Kim, T.-S.; Song, O.-K. *Appl. Phys. Lett.* **2005**, *87*, 063502.
(21) Chwang, A. B.; Kwong, R. C.; Brown, J. J. *Appl. Phys. Lett.* **2002**, *80*, 725.
(22) Aziz, H.; Popovic, Z. D.; Hu, N.-X. *Appl. Phys. Lett.* **2002**, *81*, 370.
(23) Aziz, H.; Popovic, Z. D.; Hu, N.-X.; Hor, A.-M.; Xu, G. *Science* **1999**, *283*, 1900.
(24) Cimrova, V.; Neher, D.; Remmers, M.; Kminek, I. *Adv. Mater.* **1998**, *10*, 676.
(25) Naka, S.; Shinno, K.; Okada, H.; Onnagawa, H.; Miyashita, K. *Jpn, J. Appl. Phys.* **1994**, *33*, L1772.
(26) Cao, Y.; Parker, I. D.; Yu, G.; Zhang, C.; Heeger, A. J. *Nature* **1999**, *397*, 414.

10.1021/cm0519582 CCC: $33.50
Published on Web 12/13/2005

modifying an emissive material with charge-transporting moieties.[37−63] Of the four strategies, chemical modification appears to be the most versatile and, hence, has been the most intensively pursued. Low-molar-mass evaporable materials have been constructed by bonding electron- or hole-conducting moieties to light-emitting conjugated molecules through π-conjugation, inevitably affecting individual functionalities. In most conjugated polymers, holes are preferentially transported over electrons. Electron transport has been improved by incorporating π-electron-deficient moieties, such as oxadiazole, triazole, triazine, and quinoxaline, as part of the polymer backbone, as the pendant, or as the end cap. In the case of blue OLEDs, hole injection is also a limiting factor because of the high ionization potentials of most blue-emitting materials. This difficulty can be overcome in part by adding a layer of poly(3,4-ethylenedioxythiophene)/poly(styrene sulfonate) (PEDOT/PSS) between the indium tin oxide (ITO) anode and the emissive polymer layer.[64] Because of its acidic nature, PEDOT/PSS was found to etch ITO, causing device instability.[65] This problem has been addressed using an alternative hole-injection material[66] or a self-assembled monolayer on the ITO anode.[67]

Because of the cost advantage, organic materials amenable to solution processing into noncrystalline films are of particular interest. Although conjugated polymers hold enormous potential in this regard, it is believed that monodisperse conjugated oligomers with a relatively low molecular weight are advantageous from both the scientific and technological perspectives. Monodisperse conjugated oligomers are characterized by a well-defined and uniform molecular structure as well as superior chemical purity acquired through recrystallization and/or column chromatography. Relatively short and uniform chains are also conducive to the formation of monodomain glassy-nematic films without grain boundaries through thermal annealing under mild conditions. These intrinsic merits are imperative to furnishing fundamental insight into structure−property relationships and to improving OLED device performance, as traces of impurities could result in exciton quenching and device failure. In contrast to polymers, oligomers are less likely to undergo glass transitions to form morphologically stable glassy films. Furthermore, few monodisperse conjugated oligomers are capable of both liquid-crystalline mesomorphism and an elevated glass transition temperature, T_g, to enable the processing of morphologically stable glassy-liquid-crystalline films that resist crystallization under ambient conditions.[68−70] Recently, we reported the first examples of monodisperse glassy-nematic conjugated oligomers for the demonstration of linearly polarized full-color and white-light OLEDs.[71−74] Both the luminance yield and polarization

(27) Vaeth, K. M.; Tang, C. W. *J. Appl. Phys.* **2002**, *92*, 3447.
(28) Gong, X.; Robinson, M. R.; Ostrowski, J. C.; Moses, D.; Bazan, G. C.; Heeger, A. J. *Adv. Mater.* **2002**, *14*, 581.
(29) Niu, Y.-H.; Chen, B.; Kim, T.-D.; Liu, M. S.; Jen, A. K.-Y. *Appl. Phys. Lett.* **2004**, *85*, 5433.
(30) Yan, H.; Huang, Q.; Scott, B. J.; Marks, T. J. *Appl. Phys. Lett.* **2004**, *84*, 3873.
(31) Choong, V.-E.; Shi, S.; Curless, J.; Shieh, C.-L.; Lee, H.-C.; So, F.; Shen, J.; Yang, J. *Appl. Phys. Lett.* **1999**, *75*, 172.
(32) Yan, H.; Scott, B. J.; Huang, Q.; Marks, T. J. *Adv. Mater.* **2004**, *16*, 1948.
(33) Uchida, M.; Ohmori, Y.; Noguchi, T.; Ohnishi, T.; Yoshino, K. *Jpn. J. Appl. Phys.* **1993**, *32*, L921.
(34) Ahn, J. H.; Wang, C.; Pearson, C.; Bryce, M. R.; Petty, M. C. *Appl. Phys. Lett.* **2004**, *85*, 1283.
(35) Lee, J.-H.; Wu, C.-I.; Liu, S.-W.; Huang, C.-A.; Chang, Y. *Appl. Phys. Lett.* **2005**, *86*, 103506.
(36) Oyston, S.; Wang, C.; Hughes, G.; Batsanov, A. S.; Perepichka, I. F.; Bryce, M.; Ahn, J. H.; Pearson, C.; Petty, M. C. *J. Mater. Chem.* **2005**, *15*, 194.
(37) Li, X. C.; Cacialli, F.; Giles, M.; Gruener, J.; Friend, R. H.; Holmes, A. B.; Moratti, S. C.; Yong, T. M. *Adv. Mater.* **1995**, *7*, 898.
(38) Boyd, T. J.; Geerts, Y.; Lee, J.; Fogg, D. E.; Lavoie, G. G.; Schrock, R. R.; Rubner, M. F. *Macromolecules* **1997**, *30*, 3553.
(39) Grice, A. W.; Tajbakhsh, A.; Burn, P. L.; Bradley, D. D. C. *Adv. Mater.* **1997**, *9*, 1174.
(40) Tamoto, N.; Adachi, C.; Nagai, K. *Chem. Mater.* **1997**, *9*, 1077.
(41) Chan, L.-H.; Lee, R.-H.; Hsieh, C.-F.; Yeh, H.-C.; Chen, C.-T. *J. Am. Chem. Soc.* **2002**, *124*, 6469.
(42) Danel, K.; Huang, T.-H.; Lin, J. T.; Tao, Y.-T.; Chuen, C.-H. *Chem. Mater.* **2002**, *14*, 3860.
(43) Doi, H.; Kinoshita, M.; Okumoto, K.; Shirota, Y. *Chem. Mater.* **2003**, *15*, 1080.
(44) Thomas, K. R. J.; Lin, J. T.; Velusamy, M.; Tao, Y.-T.; Chuen, C.-H. *Adv. Funct. Mater.* **2004**, *14*, 83.
(45) Wong, K.-T.; Chen, R.-T.; Fang, F.-C.; Wu, C.-C.; Lin, Y.-T. *Org. Lett.* **2005**, *7*, 1979.
(46) Bao, Z.; Peng, Z.; Galvin, M. E.; Chandross, E. A. *Chem. Mater.* **1998**, *10*, 1201.
(47) Chung, S.-J.; Kwon, K.-Y.; Lee, S.-W.; Jin, J.-I.; Lee, C. H.; Lee, C. E.; Park, Y. *Adv. Mater.* **1998**, *10*, 1112.
(48) Peng, Z.; Bao, Z.; Galvin, M. E. *Adv. Mater.* **1998**, *10*, 680.
(49) Ding, J.; Day, M.; Robertson, G.; Roovers, J. *Macromolecules* **2002**, *35*, 3474.
(50) Huang, W.; Meng, H.; Yu, W.; Gao, J.; Heeger, A. J. *Adv. Mater.* **1998**, *10*, 593.
(51) Peng, Z.; Zhang, J. *Chem. Mater.* **1999**, *11*, 1138.
(52) Redecker, M.; Bradley, D. D. C.; Inbasekaran, M.; Wu, W. W.; Woo, E. P. *Adv. Mater.* **1999**, *11*, 241.
(53) Lee, Y.; Chen, X.; Chen, S. A.; Wei, P.; Fann, W. *J. Am. Chem. Soc.* **2001**, *123*, 2296.
(54) Miteva, T.; Meisel, A.; Knoll, W.;. Nothofer, H.-G.; Scherf, U.; Müller, D. C.; Meerholz, K.; Yasuda, A.; Neher, D. *Adv. Mater.* **2001**, *13*, 565.
(55) Liu, M. S.; Jiang, X.; Herguth, P.; Jen, A. K.-Y. *Chem. Mater.* **2001**, *13*, 3820.
(56) Wu, F.-I.; Reddy, D. S.; Shu, C.-F.; Liu, M. S.; Jen, A. K.-Y. *Chem. Mater.* **2003**, *15*, 269.
(57) Gong, X.; Ma, W.; Ostrowski, J. C.; Bechgaard, K.; Bazan, G. C.; Heeger, A. J.; Xiao, S.; Moses, D. *Adv. Funct. Mater.* **2004**, *14*, 393.
(58) Jin, S.; Kim, M.; Kim, J. Y.; Lee, K.; Gal, Y. *J. Am. Chem. Soc.* **2004**, *126*, 2474.
(59) Yu, L.-S.; Chen, S. A. *Adv. Mater.* **2004**, *16*, 744.
(60) (a) Aldred, M. P.; Eastwood, A. J.; Kelly, S. M.; Vlachos, P.; Contoret, A. E. A.; Farrar, S. R.; Mansoor, B.; O'Neill, M.; Tsoi, W. C. *Chem. Mater.* **2004**, *16*, 4928. (b) Aldred, M. P.; Contoret, A. E. A.; Farrar, S. R.; Kelly, S. M.; Mathieson, D.; O'Neill, M.; Tsoi, W. C.; Vlachos, P. *Adv. Mater.* **2005**, *17*, 1368.
(61) Kwon, T. W.; Alam, M. M.; Jenekhe, S. A. *Chem. Mater.* **2004**, *16*, 4657.
(62) Chen, S.; Xu, X.; Liu, Y.; Yu, G.; Sun, X.; Qiu, W.; Ma, Y.; Zhu, D. *Adv. Funct. Mater.* **2005**, *15*, 1541.
(63) Li, Z. H.; Wong, M. S.; Tao, Y.; Lu, J. *Chem. Eur. J.* **2005**, *11*, 3285.
(64) Brown, T. M.; Kim, J. S.; Friend, R. H.; Cacialli, F.; Daik, R.; Feast, W. J. *Appl. Phys. Lett.* **1999**, *75*, 1679.
(65) de Jong, M. P.; van Ijzendoorn, L. J.; de Voigt, M. J. A. *Appl. Phys. Lett.* **2000**, *77*, 2255.
(66) Gong, X.; Moses, D.; Heeger, A. J.; Liu, S.; Jen, A. K.-Y. *Appl. Phys. Lett.* **2003**, *83*, 183.
(67) Yan, H.; Huang, Q.; Cui, J.; Veinot, J. G. C.; Kern, M. M.; Marks, T. J. *Adv. Mater.* **2003**, *15*, 835.
(68) Gill, R. E.; Meetsma, A.; Hadziioannou, G. *Adv. Mater.* **1996**, *8*, 212.
(69) Larios-López, L.; Navarro-Rodríguez, D.; Arias-Marín, E. M.; Moggio, I.; Reyes-Castañeda, C. V. *Liq. Cryst.* **2003**, *30*, 423.
(70) Güntner, R.; Farrell, T.; Scherf, U.; Miteva, T.; Yasuda, A.; Nelles, G. *J. Mater. Chem.* **2004**, *14*, 2622.
(71) Geng, Y.; Culligan, S. W.; Trajkovska, A.; Wallace, J. U.; Chen, S. H. *Chem. Mater.* **2003**, *15*, 542.
(72) Culligan, S. W.; Geng, Y.; Chen, S. H.; Klubek, K.; Vaeth, K. M.; Tang, C. W. *Adv. Mater.* **2003**, *15*, 1176.
(73) Geng, Y.; Chen, A. C. A.; Ou, J. J.; Chen, S. H.; Klubek, K.; Vaeth, K. M.; Tang, C. W. *Chem. Mater.* **2003**, *15*, 4352.
(74) Chen, A. C. A.; Culligan, S. W.; Geng, Y.; Chen, S. H.; Klubek, K.; Vaeth, K. M.; Tang, C. W. *Adv. Mater.* **2004**, *16*, 783.

Scheme 1. Synthesis of light-emitting glassy-isotropic ($n = 1$) and liquid-crystalline ($n = 3$) materials with an electron-conducting core, TRZ-F(MB)3 and TRZ-F(MB)5

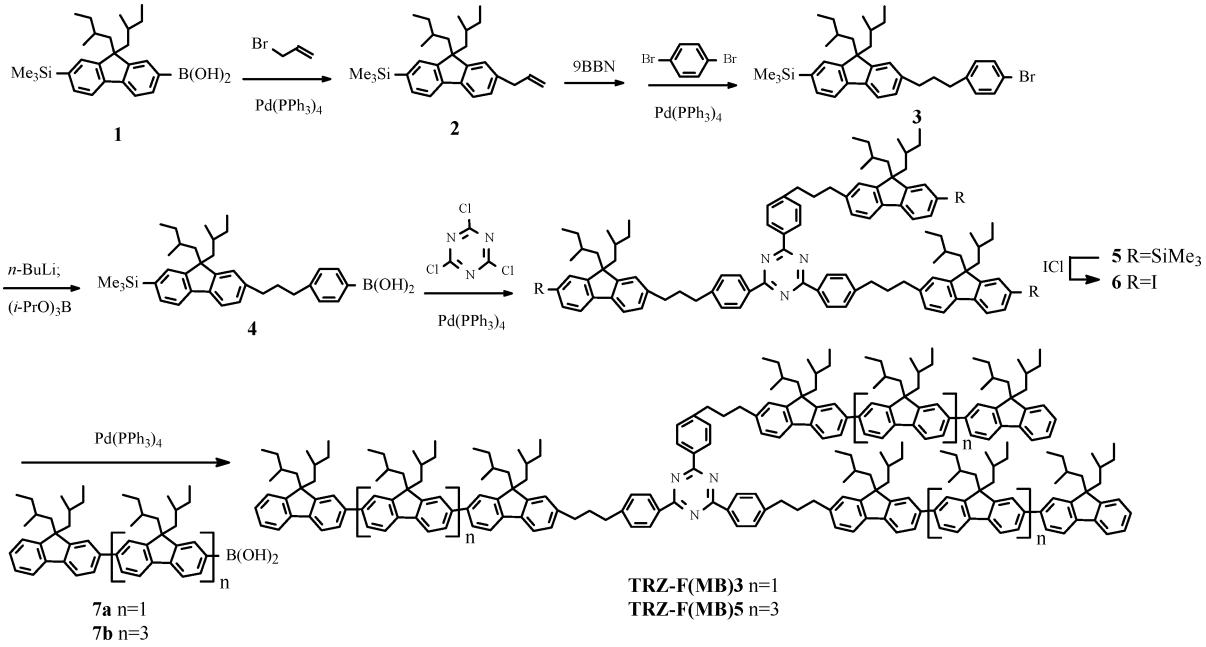

Scheme 2. Synthesis of a light-emitting glassy liquid crystal with a hole-conducting core, TPD-F(MB)5

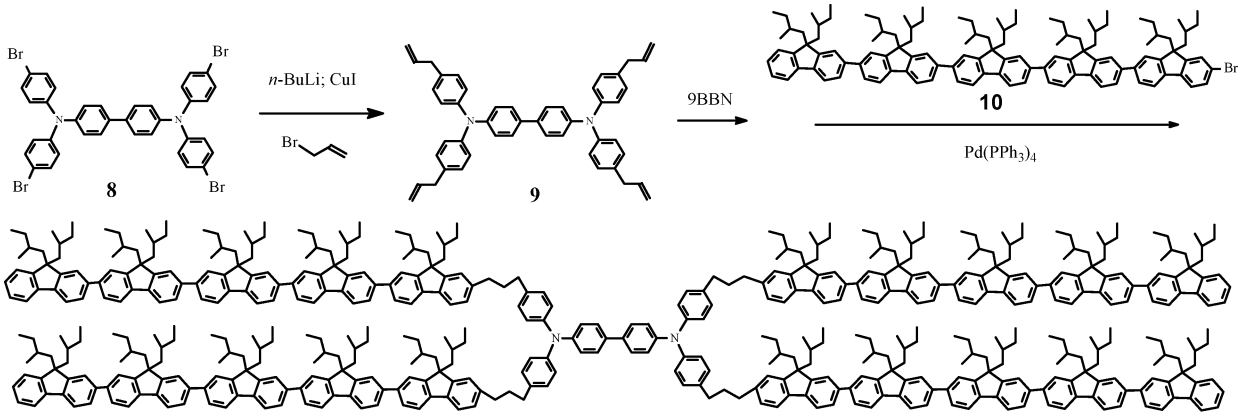

ratio are the best of all polarized OLEDs reported to date. Nevertheless, it was also recognized that charge injection and transport must be varied as desired to further improve device performance. Liquid-crystal conjugated oligomers designed for in situ polymerization represent a viable alternative to preserving molecular order in solid films; however, UV irradiation, heat, and/or initiators and inhibitors are needed for film processing.[60,75−77]

The goal of this study is to create multifunctional molecular materials capable of forming glassy-isotropic and glassy-liquid-crystalline films using light-emitting conjugated oligomers and charge injection and transport moieties as the building blocks. A flexible spacer, such as an alkyl chain, connecting the two building blocks serves to allow light emission and charge injection/transport to be incorporated without mutual interference and to prevent crystallization while encouraging glass formation of the hybrid system. Although the merits of a multilayer device structure are well-documented, multifunctional materials will offer devices comprising fewer layers, thereby reducing the fabrication costs and operating voltages while improving device performance.

II. Experimental Section

Material Synthesis and Purification Procedures. All chemicals, reagents, and solvents were used as received from commercial sources without further purification, except tetrahydrofuran (THF) and toluene, which were distilled over sodium/benzophenone. Selected target compounds were synthesized and purified according to Schemes 1−3 following the procedures outlined below. Intermediates **1**, **7a**, **7b**, and **8**−**11** as well as stand-alone terfluorene, **F(MB)3**, and pentafluorene, **F(MB)5**, were synthesized following previously reported procedures.[71,78] A literature procedure[79] was adopted for hydroboration using 9BBN followed by Suzuki coupling

(75) Jandke, M.; Hanft, D.; Strohriegl, P.; Whitehead, K.; Grell, M.; Bradley, D. D. C. *Proc. SPIE* **2001**, *4105*, 338.
(76) Contoret, A. E. A.; Farrar, S. R.; O'Neill, M.; Nicholls, J. E.; Richards, G. J.; Kelly, S. M.; Hall, A. W. *Chem. Mater.* **2002**, *14*, 1477.
(77) McCulloch, I.; Zhang, W.; Heeney, M.; Bailey, C.; Giles, M.; Graham, D.; Shkunov, M.; Sparrowe, D.; Tierney, S. *J. Mater. Chem.* **2003**, *13*, 2436.
(78) Huang, Q.; Evmenenko, G.; Dutta, P.; Marks, T. J. *J. Am. Chem. Soc.* **2003**, *125*, 14704.
(79) Bo, Z.; Qiu, J.; Li, J.; Schlueter, A. D. *Org. Lett.* **2004**, *6*, 667.

Scheme 3. Synthesis of a light-emitting glassy-isotropic material with a hole-conducting core, TPD-F(MB)3

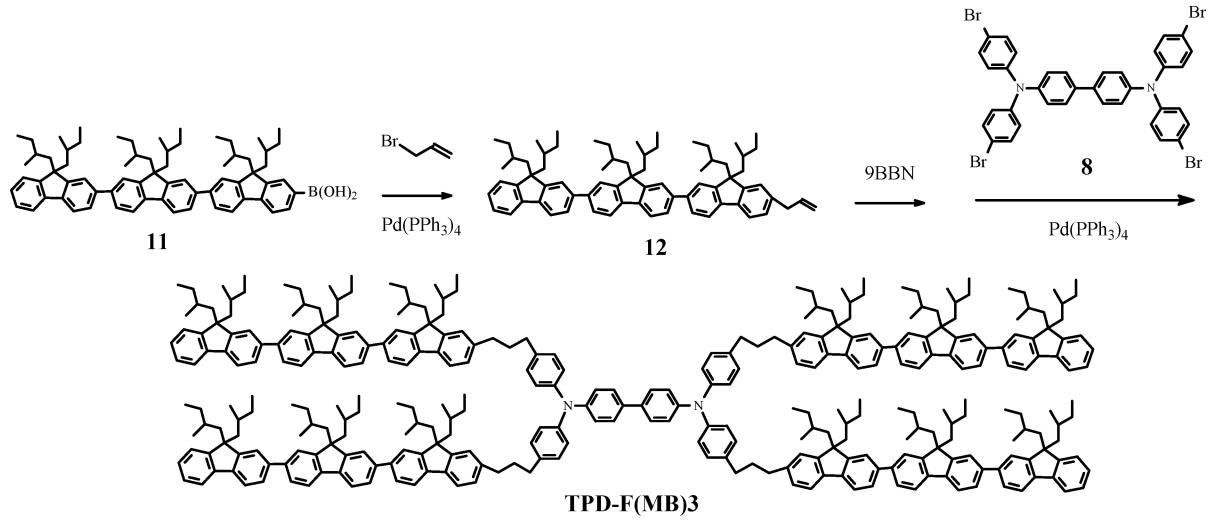

to obtain **3**, **TPD-F(MB)3**, and **TPD-F(MB)5**. According to a published procedure,[80] **5** was synthesized by Suzuki coupling of **4** with cyanuric chloride.

As indicated in Scheme 1, **TRZ-F(MB)3** and **TRZ-F(MB)5** were successfully synthesized through the use of ICl, which was found to cause undesired side reactions with the **TPD** core. Therefore, **TPD-F(MB)5** was synthesized following Scheme 2, albeit at a 10% yield, presumably because of the incomplete substitution on the tetrafunctional core, i.e., *N*,*N*,*N*′,*N*′-tetrakis-(*p*-bromophenyl)-biphenyl-4,4′-diamine (**8**), in two sequential steps. As a remedial approach, **8** was deferred until the last step in Scheme 3 for the synthesis of **TPD-F(MB)3**, resulting in a much improved yield, 58%.

2-Allyl-7-trimethylsilyl-9,9-bis(2-methylbutyl)fluorene, ***2***. Into a mixture of **1** (4.20 g, 9.94 mmol), allyl bromide (1.80 g, 14.9 mmol), K_2CO_3 (2.76 g, 20.0 mmol), and $Pd(PPh_3)_4$ (0.15 g, 0.13 mmol) were added toluene (20 mL) and H_2O (10 mL). The reaction mixture was stirred at 90 °C for 1 day and then cooled to room temperature before hexane (30 mL) was added. The organic layer was separated and washed with brine before being dried over anhydrous $MgSO_4$. Upon evaporation of the solvent, the residue was purified by column chromatography on silica gel with hexanes as the eluent to yield **2** (3.78 g, 90%) as a colorless oil. ^{1}H NMR (400 MHz, $CDCl_3$): δ (ppm) 7.65 (t, 2H), 7.47−7.54 (m, 2H), 7.14−7.28 (m, 2H), 6.00−6.10 (m, 1H), 5.06−5.09 (m, 2H), 3.47 (d, 2H), 2.08−2.13 (m, 2H), 1.84−1.89 (m, 2H), 0.82−0.93 (m, 4H), 0.56−0.61 (m, 8H), 0.24−0.31 (m, 15H).

4-Bromo-1-(3-(2-trimethylsilyl-9,9-bis(2-methylbutyl)fluoren-7-yl)propyl)-benzene, ***3***. At 0 °C, 9-BBN (0.5 M in THF, 18.2 mL, 9.10 mmol) was added to a solution of **2** (3.78 g, 9.03 mmol) in anhydrous THF (2 mL). The reaction mixture was stirred at room temperature for 30 min and then heated to 40 °C for 1 day. Upon cooling to room temperature, it was added to a mixture of 1,4-dibromobenzene (3.53 g, 15.0 mmol) in THF (10 mL), $Pd(PPh_3)_4$ (0.15 g, 0.13 mmol), and 2.0 M aqueous solution of K_2CO_3 (5.0 mL, 10.0 mmol). The reaction mixture was stirred at 90 °C for 2 days and cooled to room temperature before hexanes (30 mL) were added. The organic layer was separated and washed with brine before being dried over anhydrous $MgSO_4$. Upon evaporation of the solvent, the residue was purified by column chromatography on silica gel with hexanes as the eluent to yield **3** (3.62 g, 70%) as a colorless oil. ^{1}H NMR (400 MHz, $CDCl_3$): δ (ppm) 7.62−7.67 (m, 2H), 7.41−7.54 (m, 4H), 7.06−7.22 (m, 4H), 2.73 (t, 2H), 2.61 (t, 2H), 1.95−2.11 (m, 2H), 1.95−1.99 (m, 2H), 1.87−1.90 (m, 2H), 0.82−0.93 (m, 4H), 0.57−0.61 (m, 8H), 0.25−0.31 (m, 15H).

(3-(2-Trimethylsilyl-9,9-bis(2-methylbutyl)fluoren-7-yl)propyl)-phen-4-yl-boronic acid, ***4***. Into a solution of **3** (1.51 g, 2.62 mmol) in anhydrous THF was added *n*-BuLi (2.5 M in hexane, 1.10 mL, 2.75 mmol) at −78 °C. The reaction mixture was stirred at −78 °C for 4 h before triisopropyl borate (1.60 g, 8.51 mmol) was added in one portion. The mixture was warmed to room temperature slowly, stirred overnight, and then quenched with HCl (2.0 M, 15 mL) before a large amount of water was added for extraction with ethyl ether. The organic layer was separated and washed with brine before being dried over anhydrous $MgSO_4$. Upon evaporation of the solvent, the residue was purified by column chromatography on silica gel with hexanes/ethyl acetate (4:1) as the eluent to yield **4** (1.12 g, 70%) as a colorless powder. ^{1}H NMR (400 MHz, $CDCl_3$): δ (ppm) 8.18 (d, 2H), 7.64−7.69 (m, 2H), 7.47−7.54 (m, 2H), 7.34 (d, 2H), 7.16−7.33 (m, 2H), 2.73−2.79 (m, 4H), 2.04−2.12 (m, 4H), 1.86−1.90 (m, 2H), 0.82−0.93 (m, 4H), 0.58−0.60 (m, 8H), 0.25−0.32 (m, 15H).

2,4,6-Tris[p-(3-(2-trimethylsilyl-9,9-bis(2-methylbutyl)fluoren-7-yl)propyl)phenyl]-triazine, ***5***. A mixture of **4** (3.90 g, 7.21 mmol), cyanuric chloride (0.40 g, 2.2 mmol), $Pd(PPh_3)_4$ (0.13 g, 0.11 mmol), and Na_2CO_3 (1.80 g, 17.0 mmol) was dissolved in a mixture of toluene (15 mL) and H_2O (9 mL). The reaction mixture was stirred at 90 °C for 3 days. After the reaction mixture had cooled to room temperature, methylene chloride (30 mL) was added. The organic layer was separated and washed with brine before being dried over anhydrous $MgSO_4$. Upon evaporation of the solvent, the residue was purified by column chromatography on silica gel with hexanes/methylene chloride (2:1) as the eluent to yield **5** (1.98 g, 58%) as a white solid. ^{1}H NMR (400 MHz, $CDCl_3$): δ (ppm) 8.70 (d, 6H), 7.67 (t, 6H), 7.47−7.50 (m, 6H), 7.39 (d, 6H), 7.17−7.23 (m, 6H), 2.78 (t, 12H), 2.07−2.16 (m, 12H), 1.87−1.90 (m, 6H), 0.81−0.94 (m, 12H), 0.56−0.62 (m, 24H), 0.24−0.31 (m, 45H).

2,4,6-Tris[p-(3-(2-iodo-9,9-bis(2-methylbutyl)fluoren-7-yl)propyl)phenyl]-triazine, ***6***. Into a solution of **5** (0.53 g, 0.34 mmol) in CCl_4 (10 mL) was added ICl (1.0 M in methylene chloride, 1.50 mL, 1.50 mmol) dropwise at 0 °C. After the mixture had been stirred at room temperature for 1 h, an aqueous solution of $Na_2S_2O_3$ (10 wt %, 30 mL) was poured into the reaction mixture with vigorous stirring until discoloration for extraction with methylene chloride (15 mL). The organic layer was separated and washed with brine before being dried over anhydrous $MgSO_4$. Upon evaporation of the solvent, the residue was purified by column chromatography

(80) Janietz, D.; Bauer, M. *Synthesis* **1993**, *1993*, 33.

on silica gel with hexanes/methylene chloride (2:1) as the eluent to yield a white solid (0.40 g, 68%). ^{1}H NMR (400 MHz, $CDCl_3$): δ (ppm) 8.70 (d, 6H), 7.60−7.73 (m, 9H), 7.44 (d, 3H), 7.38 (d, 6H), 7.17−7.20 (m, 6H), 2.78 (t, 12H), 2.03−2.09 (m, 12H), 1.81−1.86 (m, 6H), 0.82−0.93 (m, 12H), 0.57−0.65 (m, 24H), 0.25−0.34 (m, 18H).

2,4,6-Tris[p-(3-(ter(9,9-bis(2-methylbutyl)fluoren-7-yl))propyl)-phenyl]-triazine, ***TRZ-F(MB)3***. Into a mixture of **6** (0.40 g, 0.23 mmol), **7a** (0.90 g, 1.4 mmol), $Pd(PPh_3)_4$ (20 mg, 0.020 mmol), and Na_2CO_3 (0.29 g, 2.7 mmol) were added toluene (2 mL) and H_2O (0.5 mL). The reaction mixture was stirred at 90 °C for 2 days. After the reaction mixture had cooled to room temperature, methylene chloride (30 mL) was added. The organic layer was separated and washed with brine before being dried over anhydrous $MgSO_4$. Upon evaporation of the solvent, the residue was purified by column chromatography on silica gel with hexanes/methylene chloride (2:1) as the eluent to yield **TRZ-F(MB)3** (0.45 g, 62%) as a white solid. ^{1}H NMR (400 MHz, $CDCl_3$): δ (ppm) 8.73 (d, 6H), 7.75−7.83 (m, 15H), 7.62−7.70 (m, 27H), 7.35−7.43 (m, 15H), 7.21−7.27 (m, 6H), 2.82 (t, 12H), 2.10−2.25 (m, 24H), 1.94−1.98 (m, 18H), 0.61−1.01 (m, 108H), 0.34−0.40 (m, 54H). Molecular weight calcd for $C_{237}H_{285}N_3$: 3175.9. MALDI/TOF MS (DCTB) *m/z* ($[M]^+$): 3173. Anal. Calcd for $C_{237}H_{285}N_3$: C, 89.63; H, 9.05; N, 1.32. Found: C, 89.53; H, 9.00; N, 1.37.

2,4,6-Tris[p-(3-(penta(9,9-bis(2-methylbutyl)fluoren-7-yl))propyl)phenyl]-triazine, ***TRZ-F(MB)5***. The procedure for the synthesis of **TRZ-F(MB)3** was followed to prepare **TRZ-F(MB)5** from **6** and **7b** as a white solid in 43% yield (70 mg). ^{1}H NMR (400 MHz, $CDCl_3$): δ (ppm) 8.73 (d, 6H), 7.36−7.86 (m, 78H), 7.31−7.43 (m, 15H), 7.21−7.23 (m, 6H), 2.82 (t, 12H), 2.11−2.27 (m, 36H), 1.93−1.97 (m, 30H), 0.63−1.01 (m, 180H), 0.34−0.43 (m, 90H). Molecular weight calcd for $C_{375}H_{453}N_3$: 5002.7. MALDI/TOF MS (DCTB) *m/z* ($[M]^+$): 5002. Anal. Calcd for $C_{375}H_{453}N_3$: C, 90.03; H, 9.13; N, 0.84. Found: C, 89.89; H, 8.84; N, 0.74.

N,N,N′,N′-Tetrakis[p-(3-(penta(9,9-bis(2-methylbutyl)fluoren-7-yl))propyl)phenyl]-biphenyl-4,4′-diamine, ***TPD-F(MB)5***. Into a solution of **9** (92 mg, 0.14 mmol) in anhydrous THF (1 mL) was added 9-BBN (0.5 M in THF, 1.25 mL, 0.625 mmol) at 0 °C. The reaction mixture was stirred at room temperature for 30 min and then heated to 40 °C for 1 day. Upon cooling to room temperature, it was added to a mixture of **10** (1.0 g, 0.57 mmol) in THF (3 mL), $Pd(PPh_3)_4$ (7 mg, 0.006 mmol), and a 2.0 M aqueous solution of K_2CO_3 (2 mL, 4.0 mmol). The reaction mixture was stirred at 90 °C for 2 days. After the reaction mixture had cooled to room temperature, methylene chloride (30 mL) was added. The organic layer was separated and washed with brine before being dried over anhydrous $MgSO_4$. After evaporation of the solvent, the residue was purified by column chromatography on silica gel with hexanes/methylene chloride (2:1) as the eluent to yield **TPD-F(MB)5** as a white solid (100 mg, 10%). ^{1}H NMR (400 MHz, $CDCl_3$): δ (ppm) 7.76−7.85 (m, 40H), 7.62−7.68 (m, 64H), 7.31−7.45 (m, 16H), 7.10−7.25 (m, 28H), 2.80 (t, 8H), 2.65 (s, 8H) 2.13−2.27 (m, 48H), 1.91−2.02 (m, 40H), 0.62−1.01 (m, 240H), 0.34−0.40 (m, 120H). Molecular weight calcd for $C_{508}H_{612}N_2$: 6746.5. MALDI/TOF MS (DCTB) *m/z* ($[M]^+$): 6746. Anal. Calcd for $C_{508}H_{612}N_2$: C, 90.44; H, 9.14; N, 0.42. Found: C, 90.37; H, 9.09; N, 0.39.

2-Allyl-ter(9,9-bis(2-methylbutyl))fluorene, ***12***. The procedure for the synthesis of **2** was followed to prepare **12** from **11** as a white solid in 87% yield (0.61 g). ^{1}H NMR (400 MHz, $CDCl_3$): δ (ppm) 7.84−7.61 (m, 5H), 7.60−7.69 (m, 9H), 7.32−7.43 (m, 3H), 7.18−7.23 (m, 2H), 6.00−6.10 (m, 1H), 5.09 (d, 2H), 3.49 (d, 2H), 2.14−2.29 (m, 6H), 1.88−1.98 (m, 6H), 0.60−0.99 (m, 36H), 0.36−0.42 (m, 18H).

N,N,N′,N′-Tetrakis[p-(3-(ter(9,9-bis(2-methylbutyl)fluoren-7-yl))-propyl)phenyl]-biphenyl-4,4′-diamine, ***TPD-F(MB)3.*** Into a solution of **12** (0.55 g, 0.58 mmol) in anhydrous THF (1 mL) was added 9-BBN (0.5 M in THF, 1.21 mL, 0.61 mmol) at 0 °C. The reaction mixture was stirred at room temperature for 30 min, and then heated to 40 °C for 1 day. Upon cooling to room temperature, it was added to a mixture of **8** (93 mg, 0.12 mmol) in THF (3 mL), $Pd(PPh_3)_4$ (6.5 mg, 0.0058 mmol), and a 2.0 M aqueous solution of K_2CO_3 (2 mL, 4 mmol). The reaction mixture was stirred at 90 °C for 2 days. After the reaction mixture had cooled to room temperature, methylene chloride (30 mL) was added. The organic layer was separated and washed with brine before being dried over $MgSO_4$. After evaporation of the solvent, the residue was purified by column chromatography on silica gel with hexanes/methylene chloride (2:1) as the eluent to yield **TPD-F(MB)3** (0.29 g, 58%) as a white solid. ^{1}H NMR (400 MHz, $CDCl_3$): δ (ppm) 7.76−7.84 (m, 20H), 7.62−7.70 (m, 36H), 7.31−7.41 (m, 16H), 7.10−7.25 (m, 28H), 2.80 (t, 8H), 2.65 (s, 8H) 2.16−2.25 (m, 32H), 1.91−2.04 (m, 24H), 0.65−1.01 (m, 144H), 0.34−0.40 (m, 72H). Molecular weight calcd for $C_{324}H_{388}N_2$: 4310.7. MALDI/TOF MS (DCTB) *m/z* ($[M]^+$): 4310. Anal. Calcd for $C_{324}H_{388}N_2$: C, 90.28; H, 9.07; N, 0.65. Found: C, 90.25; H, 9.10; N, 0.63.

Ter[9,9-bis(2-methylbutyl)fluorene], ***F(MB)3***. ^{1}H NMR (400 MHz. $CDCl_3$): δ (ppm) 7.76−7.84 (m, 5H), 7.62−7.69 (m, 9H), 7.28−7.55 (m, 6H), 2.13−2.25 (m, 6H), 1.89−2.00 (m, 6H), 0.63−0.91 (m, 36H), 0.34−0.39 (m, 18H). Molecular weight calcd for $C_{69}H_{86}$: 915.4. MALDI/TOF MS (DCTB) *m/z* ($[M]^+$): 914.7. Anal. Calcd for $C_{69}H_{86}$: C, 90.53; H, 9.47. Found: C, 90.42; H, 9.60.

Penta[9,9-bis(2-methylbutyl)fluorene], ***F(MB)5***. ^{1}H NMR (400 MHz, $CDCl_3$): δ (ppm) 7.82−7.87 (m, 6H), 7.82(d, J = 8.10 Hz, 2H), 7.77 (d, J = 7.35 Hz, 2H), 7.62−7.74 (m, 16H), 7.30−7.48 (m, 6H), 2.17−2.31 (m, 10H), 1.90−2.01 (m, 10H), 0.55−1.10 (m, 60H), 0.32−0.43 (m, 30H). Molecular weight calcd for $C_{115}H_{142}$: 1524.4. MALDI/TOF MS (DCTB): *m/z* ($[M]^+$): 1524.1. Anal. Calcd for $C_{115}H_{142}$: C, 90.61; H, 9.39. Found: C, 90.56; H, 9.31.

Molecular Structures, Morphology, and Phase Transition Temperatures. ^{1}H NMR spectra were acquired in $CDCl_3$ with an Avance-400 spectrometer (400 MHz). Elemental analysis was carried out by Quantitative Technologies, Inc. Molecular weights were measured with a TofSpec2E MALDI/TOF mass spectrometer (Micromass, Inc., Manchester, U.K.). Thermal transition temperatures were determined by differential scanning calorimetry (Perkin-Elmer DSC-7) with a continuous N_2 purge at 20 mL/min. Samples were preheated to 260 °C and then cooled at −20 °C/min to −30 °C before the reported second heating scans were recorded at 20 °C/min. Thermotropic properties were characterized with a polarizing optical microscope (DMLM, Leica, FP90 central processor and FP82 hot stage, Mettler Toledo).

Absorption and Fluorescence Spectra in Dilute Solution. Dilute solutions of oligofluorenes in chloroform were prepared at a concentration of 2×10^{-6} M. Absorption spectra were gathered with an HP 8453E UV−vis−NIR diode array spectrophotometer. Fluorescence spectra were collected with a spectrofluorimeter (Quanta Master C-60SE, Photon Technology International) at an excitation wavelength of 360 nm in a 90° orientation.

Preparation and Characterization of Neat Films. Optically flat fused silica substrates (25.4 mm diameter × 3 mm thickness, transparent to 200 nm, Esco Products) were coated with a thin film of a commercial polyimide alignment layer (Nissan SUNEVER) and uniaxially rubbed. Glassy-isotropic films were prepared by spin coating from 0.5 wt % solutions in chloroform at 4000 rpm and then dried in vacuo overnight. For the preparation of monodomain films, thermal annealing was performed in the nematic fluid temperature range to facilitate molecular orientation for 20 min with

subsequent quenching to room temperature. Polarizing optical microscopy revealed that the resulting glassy-liquid-crystalline films were defect-free under a magnification factor of 500. Films for electron diffraction were prepared under the same conditions except on NaCl substrates (International Crystal Laboratories) floated off in distilled water. Electron diffraction was performed on a transmission electron microscope (JEM 2000 EX, JEOL USA) with an accelerating voltage of 200 kV.

Polarized absorption and fluorescence were characterized using a UV−vis−NIR spectrophotometer (Lambda-900, Perkin-Elmer) and a spectrofluorimeter (Quanta Master C-60SE, Photon Technology International), respectively, following the procedures as described elsewhere.[71] Variable-angle spectroscopic ellipsometry (J. A. Woollam, V−VASE) was used to determine anisotropic refractive indices and absorption coefficients as well as film thickness following the literature procedures.[81] The film thicknesses of all four representative materials prepared under the same conditions turned out to be 50 ± 2 nm. Refractive indices were used to evaluate photoluminescence quantum yield following the procedure reported previously.[71]

Electrochemical Characterization. Cyclic voltammetry (CV) measurements were conducted using an EC-Epsilon potentiostat (Bioanalytical Systems Inc.). A silver/silver chloride wire (2-mm diameter), a platinum wire (0.5-mm diameter), and a platinum disk (1.6-mm diameter) were used as the reference, counter, and working electrodes, respectively. All oxidation scans were measured for 2.5 × 10^{-4} M solutions in anhydrous CH_2Cl_2 with 0.1 M tetraethylammonium tetrafluoroborate as the supporting electrolyte, and all the reduction scans were measured for 2.5 × 10^{-4} M solutions in anhydrous THF with tetrabutylammonium perchlorate as the supporting electrolyte. Ferrocene was used as an external standard with an oxidation potential at 0.68 V vs Ag/AgCl in THF and 0.46 V vs Ag/AgCl in CH_2Cl_2. Energy levels were measured relative to the ferrocene's HOMO level of 4.8 eV.[82]

III. Results and Discussion

Glassy-nematic conjugated oligomers have been demonstrated for polarized OLEDs,[71−74] which are potentially useful as an efficient light source for liquid-crystal displays, electroluminescent displays with improved viewing quality, projection displays, stereoscopic imaging systems, and low-threshold solid-state organic lasers with an added advantage of high polarization. Nematic oligomeric pendants can be chemically bonded to a volume-excluding core to form morphologically stable glassy liquid crystals for polarized OLEDs following a versatile core−pendant approach that has found general applicability.[83−90] Depicted in Chart 1 are the molecular structures of the target compounds synthesized for the present study. In addition to liquid-crystalline conjugated oligomers, shorter oligomeric pendants can be used to yield glassy-isotropic materials for unpolarized OLEDs. The selection of a hole- and electron-conducting core is dictated by the HOMO and LUMO energy levels as well as the charge-carrier mobility.[91−98] The phase transition temperatures included in Chart 1 were determined by differential scanning calorimetry at a heating rate of 20 °C/min.

The DSC data accompanying the molecular structures indicate that chemically attaching terfluorene and pentafluorene to a hole- and electron-conducting core has resulted in an elevation in T_g over 30 °C and in T_i by at least 55 °C in comparison to the stand-alone oligofluorene. Moreover, the absence of a phase transition involving crystals in heating and cooling scans, as shown in Figure 1, and after extended thermal annealing at temperatures above T_g observed by polarizing optical microscopy demonstrates morphological stability against thermally activated crystallization of the glassy-isotropic and liquid-crystalline materials.

Mesophase identification was accomplished by a combination of the disclinations observed under hot-stage polarizing optical microscopy and the enthalpy of transition from smectic C to nematic mesomorphism.[99] Optical micrographs, as shown in the Supporting Information, were collected on samples contained between a microscope slide and a cover slip without alignment treatment. Both **TRZ-F(MB)5** and **TPD-F(MB)5** exhibited fan-shaped textures and schlieren textures with four-point singularities expected of smectic C mesomorphism (Figures S-11 and -15) in addition to nematic mesomorphism manifested in schlieren textures with both two- and four-point singularities (Figures S-9 and -13). The DSC analysis revealed that the smectic C to nematic transition was accompanied by an enthalpy change of 1.6 and 1.2 kJ/mol of pentafluorene groups for **TRZ-F(MB)5** and **TPD-F(MB)5**, respectively; these values are consistent with the mesophase assignment.[99b] Thermal annealing of these samples in the nematic temperature regime followed by quenching to room temperature was demonstrated to be capable of preserving in the glassy state the schlieren textures characteristic of nematic or a mixture of nematic and smectic C mesomorphism (note the two- and four-point singularities in Figures S-10 and -14). For further analysis by electron diffraction, spin-coated films on bare sodium chloride substrates were thermally annealed in the nematic regime

(81) Schubert, M.; Rheinländer, B.; Cramer, C.; Schmiedel, H.; Woollam, J. A.; Herzinger, C. M.; Johs, B. *J. Opt. Soc. Am. A* **1996**, *13*, 1930.
(82) Fink, R.; Heischkel, Y.; Thelakkat, M.; Schmidt, H.-W.; Jonda, C.; Hüppauff, M. *Chem. Mater.* **1998**, *10*, 3620.
(83) Chen, S. H.; Shi, H.; Conger, B. M.; Mastrangelo, J. C.; Tsutsui, T. *Adv. Mater.* **1996**, *8*, 998.
(84) Chen, S. H.; Katsis, D.; Schmid, A. W.; Mastrangelo, J. C.; Tsutsui, T.; Blanton, T. N. *Nature* **1999**, *397*, 506.
(85) Fan, F. Y.; Culligan, S. W.; Mastrangelo, J. C.; Katsis, D.; Chen, S. H.; Blanton, T. N. *Chem. Mater.* **2001**, *13*, 4584.
(86) Katsis, D.; Chen, H. P.; Mastrangelo, J. C.; Chen, S. H.; Blanton, T. N. *Chem. Mater.* **1999**, *11*, 1590.
(87) Chen, H. P.; Katsis, D.; Mastrangelo, J. C.; Chen, S. H.; Jacobs, S. D.; Hood, P. J. *Adv. Mater.* **2000**, *12*, 1283.
(88) Chen, H. M. P.; Katsis, D.; Chen, S. H. *Chem. Mater.* **2003**, *15*, 2534.
(89) Chen, S. H.; Mastrangelo, J. C.; Jin, R. J. *Adv. Mater.* **1999**, *11*, 1183.
(90) Chen, S. H.; Chen, H. M. P.; Geng, Y.; Jacobs, S. D.; Marshall, K. L.; Blanton, T. N. *Adv. Mater.* **2003**, *15*, 1061.
(91) Strohriegl, P.; Grazulevicius, J. V. *Adv. Mater.* **2002**, *14*, 1439.
(92) Getautis, V.; Paliulis, O.; Gaidelis, V.; Jankauskas, V.; Sidaravièius, J. *J. Photochem. Photobiol. A* **2002**, *151*, 39.
(93) Yasuda, T.; Yamaguchi, Y.; Zou, D.-C.; Tsutsui, T. *Jpn. J. Appl. Phys.* **2002**, *41*, 5626.
(94) Ishi-i, T.; Yaguma, K.; Thiemann, T.; Yashima, M.; Ueno, K.; Mataka, S. *Chem. Lett.* **2004**, *33*, 1244.
(95) Kido, J.; Ohtaki, C.; Hongawa, K.; Okuyama, K.; Nagai, K. *Jpn. J. Appl. Phys.* **1993**, *32*, L917.
(96) Sainova, D.; Miteva, T.; Nothofer, H. G.; Scherf, U.; Glowacki, I.; Ulanski, J.; Fujikawa, H.; Neher, D. *Appl. Phys. Lett.* **2000**, *76*, 1810.
(97) Tao, S.; Hong, Z.; Peng, Z.; Ju, W.; Zhang, X.; Wang, P.; Wu, S.; Lee, S. *Chem. Phys. Lett.* **2004**, *397*, 1.
(98) Kulkarni, A. P.; Tonzola, C. J.; Babel, A.; Jenekhe, S. A. *Chem. Mater.* **2004**, *16*, 4556.
(99) (a) Dierking, I. *Textures of Liquid Crystals*; Wiley−VCH GmbH & Co. KGaA: Weinheim, Germany, 2003; pp 51, 99. (b) Gray, G. W.; Goodby, J. W. G. *Smectic Liquid Crystals: Textures and Structures*; Leonard Hill: London, 1984; p 66.

Chart 1. Representative Blue-Emitting Glassy-Isotropic and Glassy-Liquid-Crystalline Materials as Well as Stand-Alone Terfluorene and Pentafluorene[a]

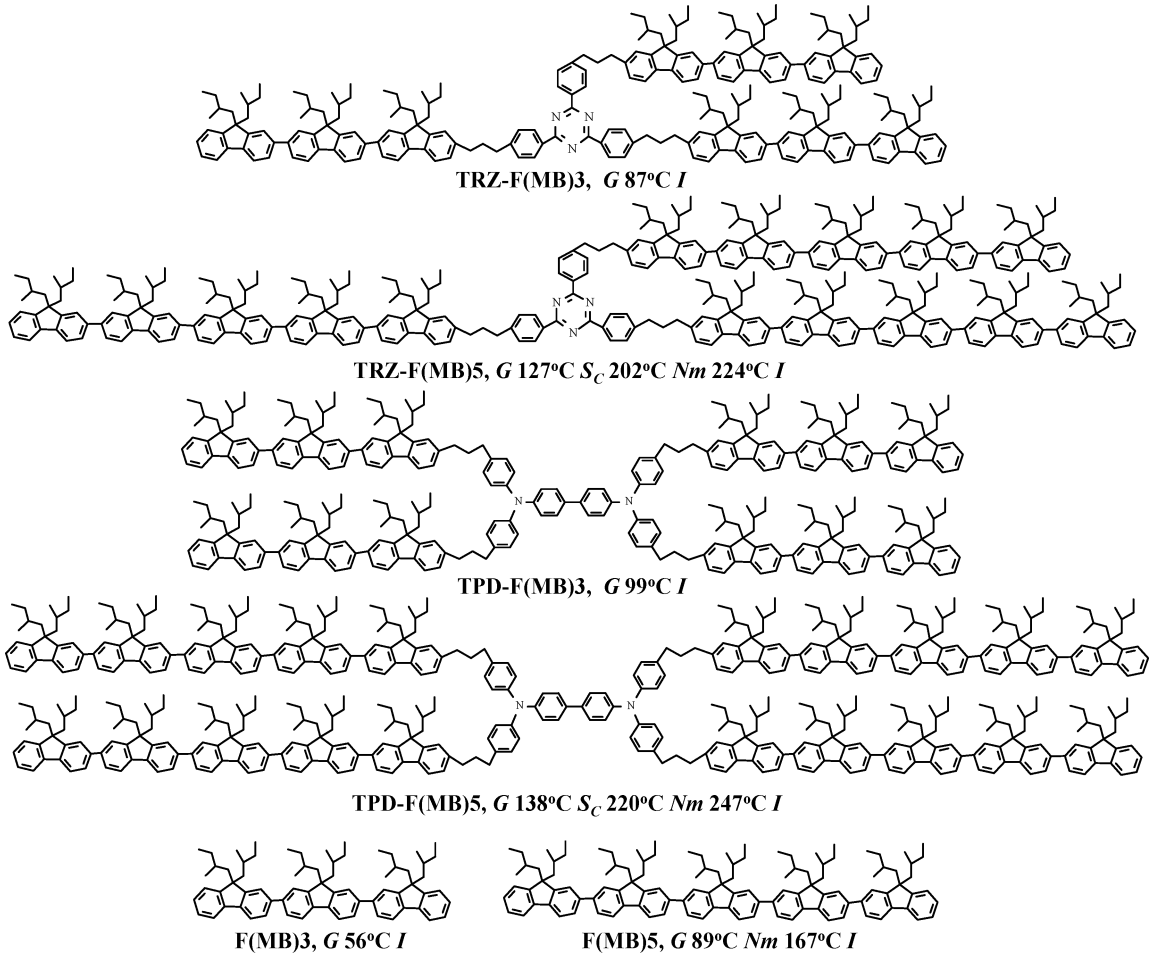

[a] *G*, glassy; *Nm*, nematic; S_C, smectic C; *I*, isotropic.

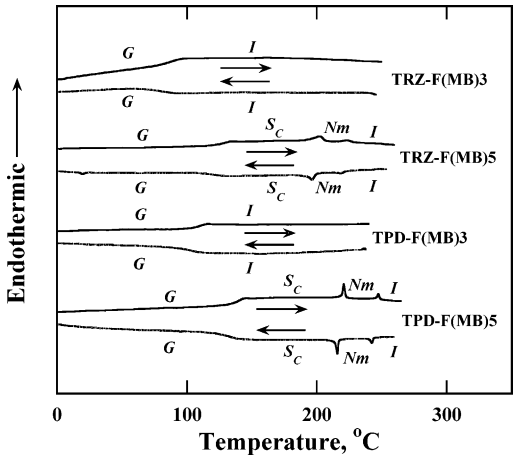

Figure 1. DSC thermograms at ±20 °C/min of samples preheated to 260 °C followed by cooling to −30 °C; G, glassy; Nm, nematic; S_C, smectic C; I, isotropic.

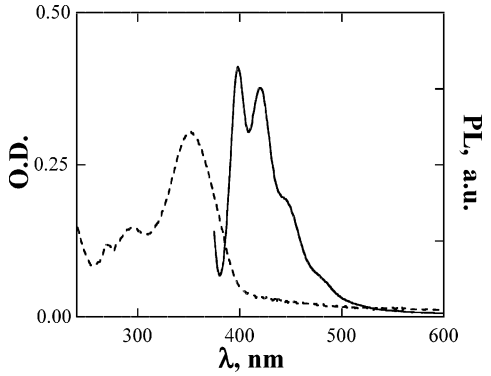

Figure 2. UV−vis absorption (dashed curve) and photoluminescence (solid curve, with 360-nm excitation) spectra of a 50-nm-thick glassy-isotropic film of **TRZ-F(MB)3**.

before being quenched through the smectic regime to room temperature. As illustrated in Figure S-17 for **TPD-F(MB)-5**, the diffraction pattern consists of a sharp inner ring and a diffuse outer ring, characteristic of the smectic layering and the nematic- or amorphous-like molecular order.[100] For the characterization of polarized light absorption and emission, monodomain (i.e., disclination-free) films were prepared on alignment-treated fused silica substrates following the same thermal treatment. Judging from the mesophase identification results as described above, it is expected that these monodomain films comprise a mixture of nematic and smectic C ordering without observable discilinations, which are referred to as glassy-liquid-crystalline films. It is noted in passing that thermal annealing in the smectic regime yielded less-ordered films because of the higher melt viscosity than encountered in the nematic regime.

(100) (a) Voigt-Martin, I. G.; Durst, H.; Reck, B.; Ringsdorf, H. *Macromolecules* **1988**, *21*, 1620. (b) Chao, C.-Y.; Hui, S. W.; Ho, J. T. *Phys. Rev. Lett.* **1997**, *78*, 4962.

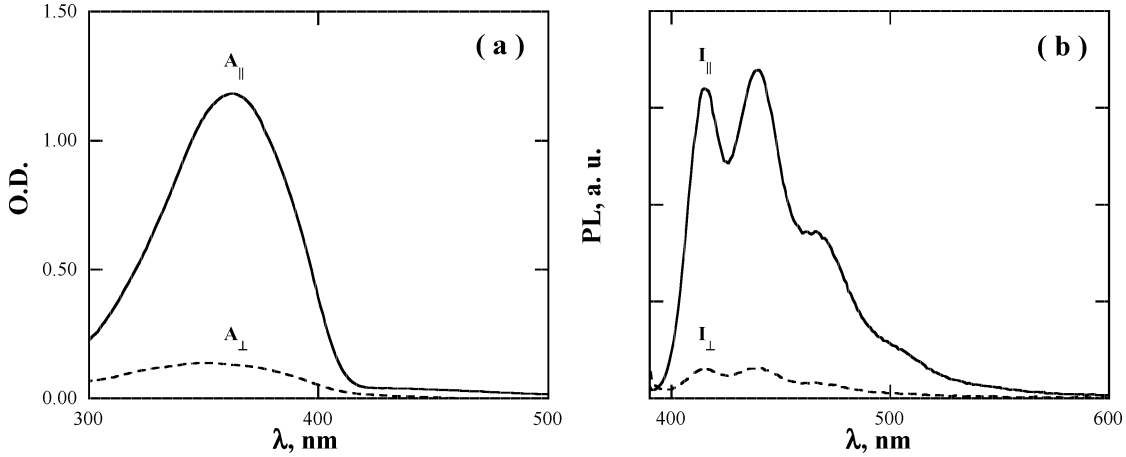

Figure 3. (a) Polarized absorption and (b) photoluminescence (with 360-nm excitation) spectra of a 50-nm-thick uniaxially aligned glassy-liquid-crystalline film of **TRZ-F(MB)5**. Symbols A and I represent absorbance and emission intensity, respectively; subscripts || and ⊥ represent directions parallel and perpendicular, respectively, to the director defined by rubbing.

The UV−vis absorption and fluorescence spectra of a 50-nm-thick glassy-isotropic film of **TRZ-F(MB)3** are shown in Figure 2. Similar spectra were obtained for an isotropic film of **TPD-F(MB)3**. As shown in the Supporting Information, there was rather insignificant spectral shifting or peak broadening of glassy-isotropic and glassy-liquid-crystalline films from dilute solutions for all four compounds, suggesting the absence of molecular aggregation in neat glassy films. A 50-nm-thick glassy-liquid-crystalline film of **TRZ-F(MB)5** was characterized as monodomain in the absence of disclinations under polarizing optical microscopy, as elaborated elsewhere for a spin-cast heptafluorene film.[101] The absorption and fluorescence spectra of the glassy-liquid-crystalline film of **TRZ-F(MB)5** are shown in Figure 3.

The absorption dichroism yields an orientational order parameter, $S = 0.75$, indicating a high degree of uniaxial alignment adopted by the pentafluorene pendants despite the presence of a trifunctional core. In fact, the observed S value is the same as for stand-alone pentafluorene.[71] A dichroic ratio of 11.2 at the emission maximum achieved with the glassy-liquid-crystalline film of **TRZ-F(MB)5** is slightly higher than that of **F(MB)5**.[71] Similar observations were made of a glassy-liquid-crystalline film of **TPD-F(MB)5**. These glassy-liquid-crystalline films hold promise for the fabrication of polarized OLEDs that might find use as the backlights for liquid-crystal displays and as electroluminescent displays with superior viewing quality. It is further noted that a longer oligofluorene pendant is expected to yield a higher emission dichroism.

Both the glassy-isotropic and glassy-liquid-crystalline films of the four representative materials were also characterized for photoluminescence quantum yield, Φ_{PL}, using 9,10-diphenylanthracene and anthracene serving as the primary and secondary standards, respectively. For the evaluation of Φ_{PL} for glassy-liquid-crystalline films of **TRZ-F(MB)5** and **TPD-F(MB)5**, ellipsometry was employed to determine the ordinary (n_o) and extraordinary (n_e) refractive indices, from which the average refractive index was calculated as $n^2 = (2n_o^2 + n_e^2)/3$. For glassy-isotropic films of **TRZ-F(MB)3** and **TPD-F(MB)3**, n was also determined by ellipsometry. The results are illustrated in Figure 4 for **TPD-F(MB)3** and **TPD-F(MB)5**.

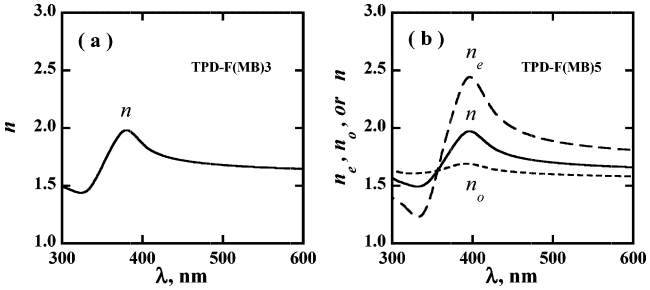

Figure 4. Refractive indices of (a) a glassy-isotropic film of **TPD-F(MB)3** and (b) a glassy-liquid-crystalline film of **TPD-F(MB)5**; similar results were obtained for **TRZ-F(MB)3** and **TRZ-F(MB)5**.

With the procedure as described previously,[71] Φ_{PL} was evaluated at 42%, 51%, 15%, and 28% for **TRZ-F(MB)3**, **TRZ-F(MB)5**, **TPD-F(MB)3**, and **TPD-F(MB)5**, respectively. Repeated measurements of Φ_{PL} indicated an experimental uncertainty of ±2% of the mean. The Φ_{PL} of a glassy-isotropic **F(MB)3** film was evaluated at 68%, and that of a glassy nematic **F(MB)5** film was reported previously to be 54%.[71] The much lower photoluminescence quantum yields of **TPD-F(MB)3** and **TPD-F(MB)5** films than those of **F(MB)3** and **F(MB)5** films, viz., 15% vs 68% and 28% vs 54%, can be attributed to energy transfer with the **TPD** core [*N*,*N*′-bis(3-methylphenyl)-*N*,*N*′-diphenylbenzidine], which was reported to have a Φ_{PL} value of 35% in glassy-isotropic film.[102]

Shown in Figure 5a are the absorption and photoluminescence spectra (with excitation at 360 nm) of **F(MB)3** and **TPD**. The two-way energy transfer between **TPD** and **F(MB)3**, the two chemical constituents of **TPD-F(MB)3**, is made possible by the overlap of the donor's emission and acceptor's absorption spectra. It is likely that the nonradiative losses accompanying the back-and-forth energy-transfer processes are responsible for the lower Φ_{PL} of a **TPD-F(MB)3** film than of the independent **F(MB)3** and **TPD** films. The same argument holds true for **TPD-F(MB)5** in

(101) Yasuda, T.; Fujita, K.; Tsutsui, T.; Geng, Y.; Culligan, S. W.; Chen, S. H. *Chem. Mater.* **2005**, *17*, 264.

(102) Mattoussi, H.; Murata, H.; Merritt, C. D.; Iizumi, Y.; Kido, J.; Kafafi, Z. *J. Appl. Phys.* **1999**, *86*, 2642.

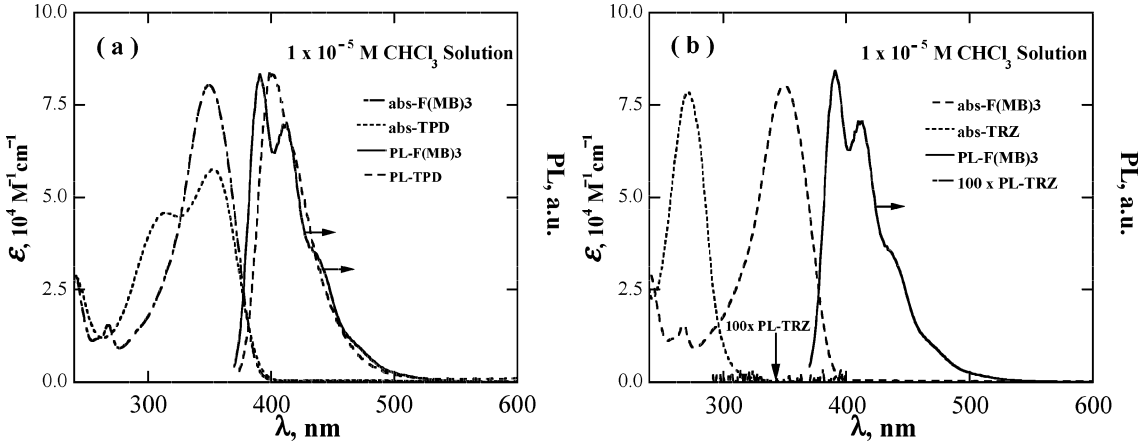

Figure 5. UV−vis absorption and photoluminescence spectra of (a) **TPD** vs **F(MB)3** and (b) **TRZ** vs **F(MB)3** for an assessment of the core−pendant energy transfer in glassy-isotropic films of **TPD-F(MB)3** and **TRZ-F(MB)3**.

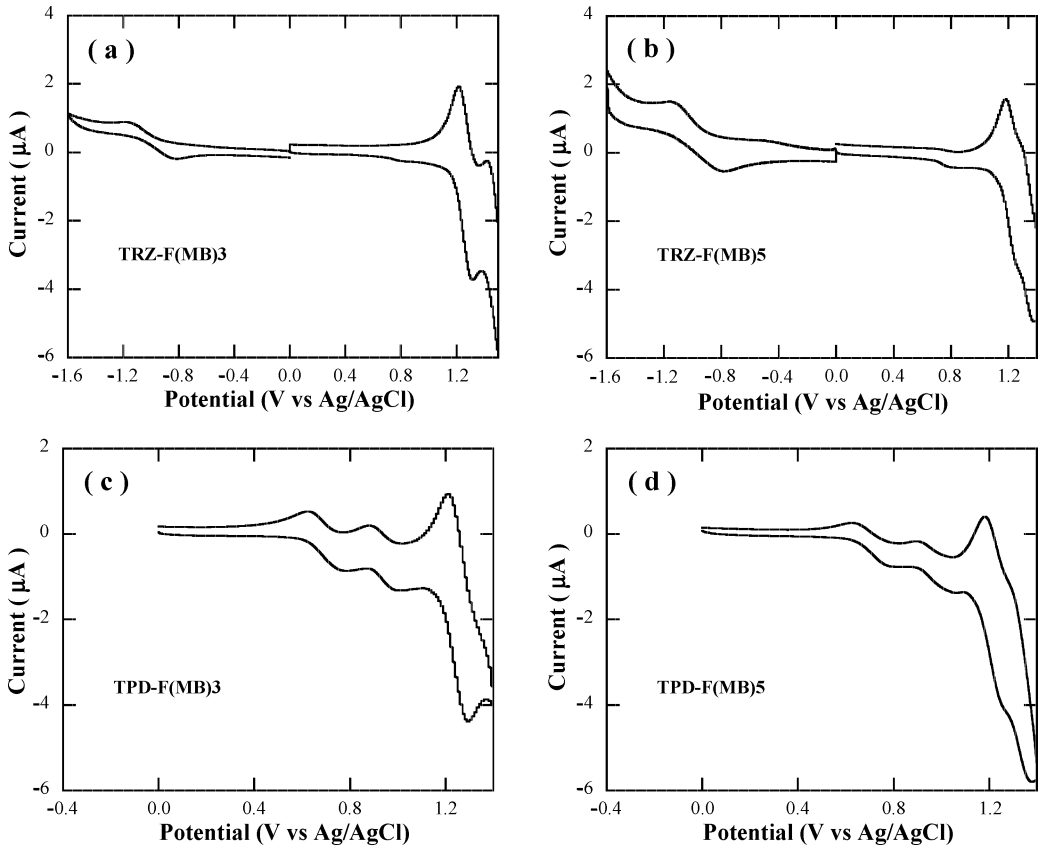

Figure 6. Cyclic voltammetric scans of (a) **TRZ-F(MB)3**, (b) **TRZ-F(MB)5**, (c) **TPD-F(MB)3**, and (d) **TPD-F(MB)5** in dilute solutions. Reduction scans of 2.5×10^{-4} M solutions in anhydrous THF with 0.1 M tetrabutylammonium perchlorate as the supporting electrolyte and oxidation scans of 2.5×10^{-4} M solutions in anhydrous CH_2Cl_2 with 0.1 M tetraethylammonium tetrafluoroborate as the supporting electrolyte.

relation to **F(MB)5**. In contrast, the **TRZ** core (2,4,6-triphenyl-1,3,5-triazine) is nonfluorescent, as shown in Figure 5b. The absorption and photoluminescence spectra presented in Figure 5b also reveal the absence of energy transfer between **TRZ** and **F(MB)3** comprising **TRZ-F(MB)3**, thereby precluding the considerable loss in Φ_{PL}. The modest losses of Φ_{PL}, however, in **TRZ-F(MB)3** and **TRZ-F(MB)-5** relative to **F(MB)3** and **F(MB)5**, respectively, namely, 42% vs 68% and 51% vs 54%, have remained unexplained.

In addition, dilute solutions of the four representative materials were characterized with cyclic voltammetry. The oxidation and reduction scans are presented in Figure 6, and the key data are summarized in Table 1.

For both **TRZ** and **TPD** cores, the pendant oligofluorenes' HOMO levels, 5.58 ± 0.03 eV, are identical to stand-alone oligofluorenes' because of the propylene spacer isolating the two structural elements. The optical band gaps of pendant terfluorene and pentafluorene are estimated at 3.20 and 3.03 eV, respectively, yielding a LUMO level of 2.38 eV for terfluorene and 2.55 eV for pentafluorene. The **TRZ** core's LUMO level of 3.12 ± 0.01 eV and the **TPD** core's HOMO level of 5.05 ± 0.01 eV are close to those reported for **TRZ**- and **TPD**-based materials.[82,103] With a HOMO level at 5.05 eV, which is close to those of PEDOT at 5.1 eV and the

(103) Adachi, C.; Nagai, K.; Tamoto, N. *Appl. Phys. Lett.* **1995**, *66*, 2679.

Table 1. Electrochemical Characterization in Dilute Solutions by Cyclic Voltammetry

compound		$E_{1/2}$(red)[a,b] vs Ag/AgCl (V)	$E_{1/2}$(ox)[a,c] vs Ag/AgCl (V)	$E_{1/2}$(red)[d] vs Fc (V)	$E_{1/2}$(ox)[d] vs Fc (V)	LUMO[e] (eV)	HOMO[e] (eV)
TRZ-F(MB)3	core	−1.01	−	−1.69	−	3.11	−
	pendant	−	1.27	−	0.81	−	5.61
TRZ-F(MB)5	core	−0.99	−	−1.67	−	3.13	−
	pendant	−	1.22	−	0.76	−	5.56
TPD-F(MB)3	core	−	0.71	−	0.25	−	5.05
	pendant	−	1.25	−	0.79	−	5.59
TPD-F(MB)5	core	−	0.72	−	0.26	−	5.06
	pendant	−	1.21	−	0.75	−	5.55

[a] Half-wave potentials, $E_{1/2}$, determined as the average of forward and reverse reduction or oxidation peaks. [b] Reduction scans of 2.5×10^{-4} M solutions in anhydrous THF with 0.1 M tetrabutylammonium perchlorate as the supporting electrolyte. [c] Oxidation scans of 2.5×10^{-4} M solutions in anhydrous CH_2Cl_2 with 0.1 M tetraethylammonium tetrafluoroborate as the supporting electrolyte. [d] Relative to ferrocene/ferrocenium with an oxidation potential at 0.68 V vs Ag/AgCl in THF and 0.46 V vs Ag/AgCl in CH_2Cl_2[82] (Fc = ferrocene). [e] Relative to ferrocene's HOMO level of 4.8 eV.[82]

ITO (indium tin oxide) anode at 4.7−5.0 eV, the **TPD** core is more receptive to hole injection than stand-alone oligofluorenes. The **TRZ** core's LUMO level at 3.12 eV is relatively close to that of the air-stable Mg/Ag cathode at 3.7 eV and, hence, is more amenable to electron injection than pendant oligofluorenes.

Inspired by recent demonstrations of improved electron and hole mobilities in functionalized conjugated polymers, the **TRZ** and **TPD** cores adopted in our material approach will enhance charge transport as desired.[59,104] Furthermore, the emission spectra shown in Figures 2 and 3 are contributed solely by pendant oligofluorenes[71] because of the cores' higher band gaps than the pendants'. In a nutshell, the new materials comprise cores intended for facile charge injection and transport and pendants designed for efficient blue emission. Used alone or as mixtures, the new materials are potentially useful for balancing the injection and transport of charges as a strategy to substantially improve OLED device efficiency and lifetime.

IV. Summary

Novel molecular systems were designed to incorporate the following features: (1) an electron- and hole-conducting core; (2) terfluorene and pentafluorene pendants for blue emission; (3) a flexible spacer attaching pendants to cores, thereby enabling independent functions of the two structural elements; (4) the ability to form glassy-isotropic and glassy-liquid-crystalline films by solution processing; and (5) tunable charge injection and transport properties while emitting unpolarized and polarized light. Four representative materials were synthesized and demonstrated to be capable of forming glassy-isotropic and glassy-liquid-crystalline films with a glass transition temperature and clearing point close to 140 and 250 °C, respectively; an orientational order parameter of 0.75; a photoluminescence quantum yield in neat film up to 51%; and HOMO and LUMO levels intermediate between blue-emitting oligofluorenes and the electrodes commonly used in OLEDs (e.g., ITO and Mg/Ag). Work is in progress to exploit these promising materials for the fabrication of highly efficient OLEDs with long-term stability, and the results will be the subject of a future publication.

Acknowledgment. The authors thank Ching W. Tang of Eastman Kodak Company and Sean W. Culligan for insightful discussions, Feng Yan for assistance in the synthesis of some intermediates, Kevin Klubek and Andrew J. Hoteling of Eastman Kodak Company for MALDI/TOF analysis, Brian McIntyre of the Institute of Optics for electron microscopy, and Kenneth L. Marshall and Stephen D. Jacobs of the Laboratory for Laser Energetics for assistance in material characterization. We are grateful for the financial support provided by the National Science Foundation under Grant CTS-0204827, Eastman Kodak Company, and the New York State Center for Electronic Imaging Systems. Additional funding was provided by the Department of Energy, Office of Inertial Confinement Fusion, under Cooperative Agreement No. DE-FC03-92SF19460 with the Laboratory for Laser Energetics and the New York State Energy Research and Development Authority. The support of DOE does not constitute an endorsement by DOE of the views expressed in this article.

Supporting Information Available: Polarizing optical micrographs, electron diffraction pattern, and UV−vis absorption and photoluminescence spectra with an unpolarized excitation at 360 nm in dilute solution and glassy-isotropic and glassy-liquid-crystalline films. These materials are available free of charge via the Internet at http://pubs.acs.org.

CM0519582

(104) Sun, R. G.; Wang, Y. Z.; Wang, D. K.; Zhang, Q. B. *Synth. Met.* **2000**, *111−112*, 403.